Proceedings of the
47th IEEE Conference on Decision and Control
Cancun, Mexico, Dec. 9-11, 2008

Feasibility Considerations in Formation Control: Phantom Track Generation through Multi-UAV Collaboration

D.H.A. Maithripala, S. Jayasuriya

Abstract— **Considered is the so called radar deception problem to motivate a change in paradigm in the approach to formation control that would address the key issue of dynamic feasibility. In this problem a team of possibly heterogeneous fixed winged Unmanned Aerial Vehicles (UAVs) cooperate to deceive a ground radar network into seeing a spurious phantom track in its radar space. A real-time motion planning algorithm is developed for this collaborating multi-agent system. At the heart of the proposed algorithm is the explicit consideration of actuator and operating constraints of the individual agents. Constrained dynamics of the multi-agent system are derived such that these constraints are transparent in the dynamic equations, to address the key issue of dynamic feasibility in formation control. Simulations are given validating the proposed approach.**

I. Introduction

Collaborating multi-agent systems have received increased attention in the recent past and have applications in exploration and mapping, search and rescue, surveillance, cooperative manipulation, automated highways and network centric warfare. Dynamic constraints that limit the maneuverability of a single agent can have a magnified effect in limiting the maneuverability of such multi-agent systems in accomplishing a prescribed group behavior. Most approaches to formation control of multi-agent systems overlook this critical aspect and the resulting reference trajectories may be dynamically infeasible for the individual agents to track. This is especially true when little flexibility is offered in satisfying the formation constraints. The formation control problem of radar deception through a collaborating team of multi-UAVs is considered to motivate a change in paradigm in formation control to address the key issue of dynamic feasibility. Here a team of fixed winged UAVs cooperate to deceive a ground radar network into seeing a spurious phantom track in its radar space. It is assumed that each UAV engaging a radar it is assigned to has the capability to intercept, introduce a time delay and re-transmit the radar's transmitted pulses thereby making the radar detect a target at a false range. It is also assumed that each UAV can remain stealth to all radars and re-transmit these delayed radar signals only to the radar it engages. The problem essentially involves all the extended lines of sight, from the radars to the UAVs engaging them, intersecting at a common point and tracing a path in space, which is a constraint on the system configuration space. The radar deception scenario is illustrated in Fig.1 for the case of four UAVs engaging a radar network having four radar stations. This problem first appeared in [1], [2] while the essential role dynamic feasibility plays in this problem was first pointed out in [3]. Subsequently this problem has been studied in [4], [5], [6], [7], [8] for the 2D scenario and the only known 3D results are in [9].

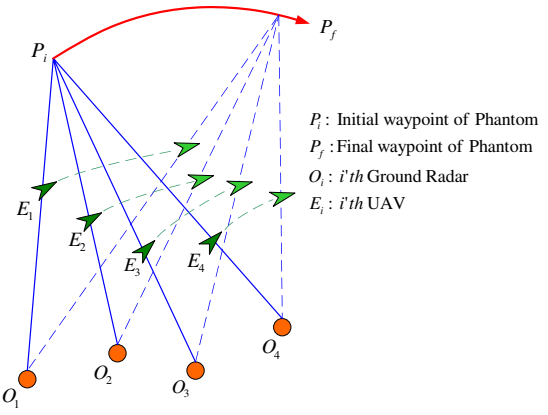

Fig. 1. Radar deception through phantom track generation.

This paper serves as an application paper to a general theory developed by the authors in [10]. Briefly, [10] presents a motion planning algorithm for a class of problems in formation control based on a unifying, intrinsic formulation of geometric constraints (including dynamic and formation constraints). Results given here are the first to successfully consider individual agent dynamics while giving real-time solutions to the radar deception problem.

The approach proposed in this paper is to embed the configuration and dynamic constraints of formation control into the design of reference trajectories to be used simultaneously by the tracking controllers of the individual agents. Theoretically (in the absence of model uncertainty, and external disturbances) this can result in zero tracking error. Based on this approach, a real-time motion planning algorithm for the radar deception problem is developed to design individual reference trajectories that can ideally result in zero formation error at the tracking control stage. In actual implementation, model uncertainty and disturbance rejection will need to be accounted through feedback at this tracking control stage. At the heart of the proposed algorithm is the explicit consideration of actuator and operating constraints of the individual agents and the derivation of constrained dynamics of the multi-agent system that makes these constraints transparent, thereby addressing the key issue of dynamic feasibility in formation control.

D.H.A. Maithripala and S. Jayasuriya are with the Department of Mechanical Engineering, Texas A&M University, College Station, TX 77843-3123, USA asanka@tamu.edu, sjayasuriya@tamu.edu

This paper is organized into four sections of which this introduction is section-I. The proposed motion planning algorithm is outlined in section-II next and forms the bulk of the presentation. Simulation results of the motion planning algorithm are given in section-III followed by concluding remarks in section-IV.

II. Proposed motion planning algorithm

Consider the case of N-UAVs engaging N-radars restricted to the 2D plane. The unicycle model is proposed to capture the dynamic, operating and actuator constraints of the UAVs. Let (x_i, y_i, θ_i) give the configuration of the ith UAV where (x_i, y_i) is the position and θ_i is its orientation. Assume an imaginary UAV whose trajectory will realistically mimic the trajectory of an actual aircraft. Let (x, y, θ) be the position and orientation of this imaginary UAV. Let $(\bar{x}_i, \bar{y}_i)$ give the position of the ith ground radar which is stationary by assumption.

The nonholonomic constraint of a unicycle representing the ith UAV is $\dot{x}_i \sin\theta_i - \dot{y}_i \cos\theta_i = 0$. Its equivalent control form along with mass and inertia effects are given by

$$\begin{aligned} \dot{x}_i &= v_i \cos\theta_i & \dot{v}_i &= \frac{1}{m_i} f_i \\ \dot{y}_i &= v_i \sin\theta_i & & \\ \dot{\theta}_i &= w_i & \dot{w}_i &= \frac{1}{J_i} \tau_i \end{aligned} \tag{1}$$

where $m_i, J_i, v_i, w_i, f_i, \tau_i$ are mass, inertia, speed, steer, force and torque of the ith UAV.

Assuming the UAV to be fixed winged, its speed v_i will have to be lower bounded to avoid stall, a flight operating constraint on the UAV. Stability of the UAV and actuator limitations will upper and lower bound the steer w_i as well as the rate of steer $\dot{w}_i$. Actuator limitations will impose an upper bound on the thrust force f_i while the maximum attainable drag force will impose a lower bound on f_i. These actuator and operating constraints are captured through

$$\begin{aligned} {v_i}^{min} \leq \;& v_i & \leq {v_i}^{max} \\ -{w_i}^{max} \leq \;& w_i & \leq {w_i}^{max} \\ -{f_i}^{min} \leq \;& f_i & \leq {f_i}^{max} \\ -{\tau_i}^{max} \leq \;& \tau_i & \leq {\tau_i}^{max} \end{aligned} \tag{2}$$

where $v_i^{max}, v_i^{min}, w_i^{max}, f_i^{min}, f_i^{max}, \tau_i^{max}$ are all positive constants. The dynamical model of the imaginary UAV representing the phantom can similarly be given by Eq.(1) and Eq.(2) with the subscript i dropped.

Next the multi-agent system is separated into N geometrically equivalent subsystems corresponding to the N radar-UAV pairs, to facilitate distributed control. Each subsystem now only has two UAVs, one representing the phantom and the other the UAV engaging the radar. Consider the ith such subsystem and call it $\mathcal{A}$. A trajectory of $\mathcal{A}$ is a curve on Q, $\gamma : [a, b] \to Q$, whose tangent vector on Q along the curve γ we denote by γ'. The configuration space of the ith subsystem, shown in Fig.2, has the structure of a manifold Q, and we assign the local coordinates $q = (x, y, \theta, x_i, y_i, \theta_i)$. On the manifold Q, $\boldsymbol{\partial_q} = \{\frac{\partial}{\partial x}, \frac{\partial}{\partial y}, \frac{\partial}{\partial \theta}, \frac{\partial}{\partial x_i}, \frac{\partial}{\partial y_i}, \frac{\partial}{\partial \theta_i}\}$ is the coordinate basis for T_qQ and $\mathbf{dq} = \{dx, dy, d\theta, dx_i, dy_i, d\theta_i, d\phi\}$

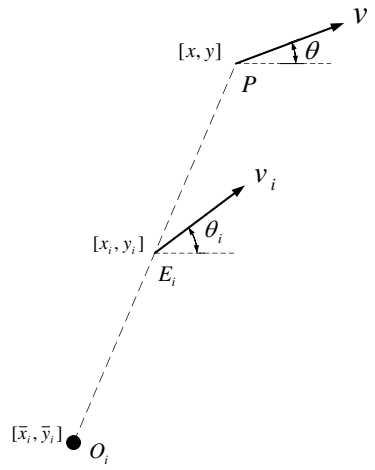

Fig. 2. Configuration of the ith subsystem.

is its dual basis for T_q^*Q. We refer the reader to [11], [12] for details of the differential geometric ideas and notation used in this paper. The Riemannian metric corresponding to the kinetic energy of the system is $\mathbb{G} = m(dx \otimes dx + dy \otimes dy) + Jd\theta \otimes \theta + m_i(dx_i \otimes dx_i + dy_i \otimes dy_i) + J_i d\theta_i \otimes \theta_i$. For computational convenience, and without loss of generality, we assume unit mass and inertia for both UAVs of $\mathcal{A}$. The inertia matrix associated with the Riemannian metric $\mathbb{G}$ is then the identity $[\mathbf{I}]_{6\times 6}$. Let us next proceed to derive the constrained dynamics of the ith subsystem $\mathcal{A}$.

Nonholonomic constraints on $\mathcal{A}$ are;

$$\begin{aligned} \dot{x}\sin\theta - \dot{y}\cos\theta &= 0 \\ \dot{x}_i \sin\theta_i - \dot{y}_i \cos\theta_i &= 0 \end{aligned} \tag{3}$$

The annihilating codistribution associated with the above nonholonomic constraints of $\mathcal{A}$ is given by;

$$\Lambda : \quad \begin{aligned} \boldsymbol{\alpha}_1 &= \sin\theta dx - \cos\theta dy \\ \boldsymbol{\alpha}_2 &= \sin\theta_i dx_i - \cos\theta_i dy_i \end{aligned}$$

The distribution Δ associated with the annihilating codistribution Λ is spanned by $\Delta = \{\mathbf{e}_v, \mathbf{e}_w, \mathbf{e}_{v_i}, \mathbf{e}_{w_i}\}$ where $\mathbf{e}_v = \cos\theta \frac{\partial}{\partial x} + \sin\theta \frac{\partial}{\partial y}$, $\mathbf{e}_w = \frac{\partial}{\partial \theta}$, $\mathbf{e}_{v_i} = \cos\theta_i \frac{\partial}{\partial x_i} + \sin\theta \frac{\partial}{\partial y_i}$, $\mathbf{e}_{w_i} = \frac{\partial}{\partial \theta_i}$ and $\Delta^\perp$, the compliment of Δ, is spanned by $\Delta^\perp = \{\mathbf{e}_z, \mathbf{e}_{z_i}\}$ where $\mathbf{e}_z = \mathbb{G}^\sharp(\boldsymbol{\alpha}_1) = \sin\theta \frac{\partial}{\partial x} - \cos\theta \frac{\partial}{\partial x}$, $\mathbf{e}_{z_i} = \mathbb{G}^\sharp(\boldsymbol{\alpha}_2) = \sin\theta_i \frac{\partial}{\partial x_i} - \cos\theta_i \frac{\partial}{\partial y_i}$. Here $\mathbb{G}^\sharp : T^*Q \to TQ$ is the isomorphism associated with the metric $\mathbb{G}$ mapping covector fields to vector fields. For a covector $\boldsymbol{\alpha} = \alpha_j dq^j$, and basis $\boldsymbol{\partial_q} = \{\frac{\partial}{\partial q^j}\}$; $\mathbb{G}^\sharp(\boldsymbol{\alpha}) = \mathbb{G}^{ij}\alpha_j \frac{\partial}{\partial q^i}$ where $\mathbb{G}^{ij}\mathbb{G}_{jk} = \delta^i_k$.

The frame of vector fields $(\mathbf{e}_v, \mathbf{e}_w, \mathbf{e}_{v_i}, \mathbf{e}_{w_i}, \mathbf{e}_z, \mathbf{e}_{z_i})$ span T_qQ on the manifold Q and hence is another basis for T_qQ. Associated with the frame $\mathbf{e} = \{\mathbf{e}_v, \mathbf{e}_w, \mathbf{e}_{v_i}, \mathbf{e}_{w_i}, \mathbf{e}_z, \mathbf{e}_{z_i}\}$ is its dual frame $\boldsymbol{\sigma} = \{\sigma^v, \sigma^w, \sigma^{v_i}, \sigma^{w_i}, \sigma^z, \sigma^{z_i}\}$. The tangent vector γ' on Q associated with a trajectory curve γ can be given in either of the frames $\boldsymbol{\partial_q}$ or $\mathbf{e}$. Note that the functions v, w, v_i, w_i of $\gamma' = v\mathbf{e}_v + w\mathbf{e}_w + v_i\mathbf{e}_{v_i} + w_i\mathbf{e}_{w_i} + z\mathbf{e}_z + z_i\mathbf{e}_{z_i}$ are the same speed and steer controls corresponding

to the dynamic models of the ith and the phantom UAV. The actuator and operating constraints acting on $\mathcal{A}$, given in Eq.(2), can be written concisely as follows

$$(\mu_i, \dot{\mu}_i) \in \Pi_i \tag{4}$$

where $\mu_i = (v, w, v_i, w_i)$ and Π_i is a compact set which does not have to have zero in its inclusion.

The requirement that the UAV has to be in-line with its corresponding radar and the phantom gives rise to a configuration constraint. The map $\mathcal{C} : Q \mapsto \mathbf{0} \in \mathcal{R}^m$ capturing this configuration constraint on $\mathcal{A}$ is

$$(x - \bar{x}_i)(y_i - \bar{y}_i) - (y - \bar{y}_i)(x_i - \bar{x}_i) = 0 \tag{5}$$

and the differential of this map, $d\mathcal{C}$, is given by the 1-form $\boldsymbol{\beta}_1 = (y_i - \bar{y}_i)dx - (x_i - \bar{x}_i)dy - (y - \bar{y}_i)dx_i + (x - \bar{x}_i)dy_i$

The intersection of the annihilating codistributions Λ and $d\mathcal{C}$ gives the unique annihilating codistribution $\Omega : \Lambda \oplus d\mathcal{C}$. The distribution $\mathcal{D}$ associated with the annihilating codistribution Ω is spanned by the vector fields; $\mathbf{x}_1 = h_i \cos\theta \frac{\partial}{\partial x} + h_i \sin\theta \frac{\partial}{\partial y} + h\cos\theta_i \frac{\partial}{\partial x_i} + h \sin\theta_i \frac{\partial}{\partial y_i}$, $\mathbf{x}_2 = \frac{\partial}{\partial \theta}$, $\mathbf{x}_3 = \frac{\partial}{\partial \theta_i}$ where $h = (x_i - \bar{x}_i)\sin\theta - (y_i - \bar{y}_i)\cos\theta$ and $h_i = (x - \bar{x}_i)\sin\theta_i - (y - \bar{y}_i)\cos\theta_i$. Vector fields $\mathbf{x}_4 = \mathbb{G}^\sharp(\alpha_1) = \sin\theta \frac{\partial}{\partial x} - \cos\theta \frac{\partial}{\partial y}$, $\mathbf{x}_5 = \mathbb{G}^\sharp(\alpha_2) = \sin\theta_i \frac{\partial}{\partial x_i} - \cos\theta_i \frac{\partial}{\partial y_i}$ and $\mathbf{x}_6 = \mathbb{G}^\sharp(\beta_1) = (y_i - \bar{y}_i)\frac{\partial}{\partial x} - (x_i - \bar{x}_i)\frac{\partial}{\partial y} - (y - \bar{y}_i)\frac{\partial}{\partial x_i} + (x - \bar{x}_i)\frac{\partial}{\partial y_i}$ span $\mathcal{D}^\perp$.

A curve $\gamma : [a, b] \mapsto Q$ is a solution of the constrained system $\mathcal{A}$ *iff* $\gamma'(t_0) \in \mathcal{D}$ and γ satisfies;

$$\overset{A}{\nabla}_{\gamma'(t)} \gamma'(t) = P\left(Y(\gamma(t))\right)$$

where $Y = \mathbb{G}^\sharp(F)$ with the 1-form F representing the force and $P : TQ \mapsto TQ$ is the $\mathbb{G}$ orthogonal projection map onto $\mathcal{D}$. The constrained connection $\overset{A}{\nabla}_{\gamma'(t)} \gamma'(t)$ is given by [13];

$$\overset{A}{\nabla}_{\gamma'(t)} \gamma'(t) = \nabla_{\gamma'(t)}\gamma'(t) + A^{-1}\left(\left(\nabla_{\gamma'(t)} A P'\right)\left(\gamma'(t)\right)\right)$$

where A can be *any* invertible matrix. A property of $\overset{A}{\nabla}$ is that it *restricts* to $\mathcal{D}$ meaning that $\overset{A}{\nabla}_{X_1} X_2 \in \mathcal{D}$ for every $X_2 \in \mathcal{D}$. Hence a solution γ of the constrained system $\mathcal{A}$ satisfies all holonomic and nonholonomic constraints captured through the distribution $\mathcal{D}$. Expression of $\overset{A}{\nabla}_{\gamma'} \gamma'$ in the two frames $\mathbf{e}$, $\boldsymbol{\partial_q}$ is as follows;

$$\overset{A}{\nabla}_{\gamma'} \gamma' = \mathbf{e}_k(\dot{v}^k + v^j \overset{A}{\omega}{}^k_j (\gamma')) = \partial_{q^k}(\ddot{q}^k + \dot{q}^j \overset{A}{\Gamma}{}^k_j (\gamma'))$$

where the connection coefficients and the connection 1-forms of $\overset{A}{\nabla}$ are defined by $\overset{A}{\nabla}_{\mathbf{e}_i} \mathbf{e}_j := \mathbf{e}_k \overset{A}{\omega}{}^k_{ij}$, $\overset{A}{\omega}{}^k_j := \overset{A}{\omega}{}^k_{rj}\, \sigma^r$ and $\overset{A}{\nabla}_{\partial_{q^i}} \partial_{q^j} := \partial_{q^k} \overset{A}{\Gamma}{}^k_{ij}$, $\overset{A}{\Gamma}{}^k_j := \overset{A}{\Gamma}{}^k_{rj}\, \partial_{q^r}$. The connection coefficients $\overset{A}{\Gamma}{}^k_{ij}$ are given by

$$\overset{A}{\Gamma}{}^i_{jk} = \overset{\mathbb{G}}{\Gamma}{}^i_{jk} + (A^{-1})^i_r \frac{\partial (AP')^r_j}{\partial q^k} + (A^{-1})^i_r \overset{\mathbb{G}}{\Gamma}{}^r_{km} (AP')^m_j - (A^{-1})^i_r \overset{\mathbb{G}}{\Gamma}{}^m_{kj} (AP')^r_m$$

We next compute P' to compute these connection coefficients $\overset{A}{\Gamma}{}^k_{ij}$. In the basis $\mathbf{x} = \{\mathbf{x}_1, \ldots, \mathbf{x}_6\}$, P' has the matrix representation $\left[P'\right]_{\mathbf{x}} = \begin{bmatrix} [0]_{3\times 3} & [0]_{3\times 3} \\ [0]_{3\times 3} & [I]_{3\times 3} \end{bmatrix}$. Let $\mathbf{x} = \boldsymbol{\partial_q}\mathcal{R}$ be the change of basis where $\mathbf{x}_i = \frac{\partial}{\partial q^j}\mathcal{R}^j_i$ and $\mathcal{R}$ is the non-singular matrix whose (i, j)th element is $\mathcal{R}^i_j$.

Matrix representation of P' in $\boldsymbol{\partial_q}$ is given by $[P']_{\boldsymbol{\partial_q}} = \mathcal{R}[P']_{\mathbf{x}}\mathcal{R}^{-1}$. The projection map P, the $\mathbb{G}$-orthogonal projection onto $\mathcal{D}$, in the basis $\boldsymbol{\partial_q}$ is simply $[P]_{\boldsymbol{\partial_q}} = I - [P']_{\boldsymbol{\partial_q}}$ where I is the identity.

We choose $A = (h^2 + h_i^2)I$ to eliminate denominator terms of P'. Since the Riemannian metric $\mathbb{G}$ is constant, $\overset{\mathbb{G}}{\Gamma}{}^i_{jk} = 0$ for $\forall\, i, j, k$ and we have

$$\overset{A}{\Gamma}{}^i_{jk} = (A^{-1})^i_r \frac{\partial (AP')^r_j}{\partial q^k} = \frac{1}{(h^2 + h_i^2)} \frac{\partial (AP')^i_j}{\partial q^k} \tag{6}$$

Since operating and actuator constraints of the UAVs are captured through the constraints $(\mu_i, \dot{\mu}_i) \in \Pi$ where $\mu_i = (v, w, v_i, w_i)$ with $\gamma' = v\mathbf{e}_v + w\mathbf{e}_w + v_i\mathbf{e}_{v_i} + w_i\mathbf{e}_{w_i} + z\mathbf{e}_z + z_i\mathbf{e}_{z_i}$ being in the frame $\mathbf{e}$, we proceed to derive the constrained dynamics of $\mathcal{A}$ in this $\mathbf{e}$ frame.

Connection coefficients $\overset{A}{\omega}{}^k_{ij}$ are computed through the following transformation rule for the matrix of connection 1-forms;

$$\overset{A}{\omega} = \mathcal{S}^{-1}\, \overset{A}{\Gamma}\, \mathcal{S} + \mathcal{S}^{-1} d\mathcal{S} \tag{7}$$

where $\mathcal{S}$ is the change of basis given by $\mathbf{e} = \boldsymbol{\partial_q}\mathcal{S}$ and $\overset{A}{\omega} := \begin{pmatrix} \overset{A}{\omega}{}^k_j \end{pmatrix}$, $\overset{A}{\Gamma} := \begin{pmatrix} \overset{A}{\Gamma}{}^k_j \end{pmatrix}$ are $n \times n$ matrices of connection 1-forms.

The force F along γ is given by the covector $F = f\sigma^v + \tau\sigma^w + f_i\sigma^{v_i} + \tau_i\sigma^{w_i}$ in the frame $\boldsymbol{\sigma}$ and its associated tangent vector field is $Y = \mathbb{G}^\sharp(F) = fe_v + \tau e_w + f_i e_{v_i} + \tau_i e_{w_i}$. Let $\mathbf{x} = \mathbf{e}\mathcal{Z}$ be the change of basis where $\mathcal{Z} = \mathcal{S}^{-1}\mathcal{R}$ with $\mathbf{x} = \boldsymbol{\partial_q}\mathcal{R}$ and $\mathbf{e} = \boldsymbol{\partial_q}\mathcal{S}$. Matrix representation of the projection map P in the $\mathbf{e}$ basis is given by $[P]_{\mathbf{e}} = \mathcal{Z}[P]_{\mathbf{x}}\mathcal{Z}^{-1}$. The projection of Y onto the distribution $\mathcal{D}$ is then given by $P(Y(\gamma)) = \frac{h_i(h_i f + h f_i)}{(h^2 + h_i^2)} e_v + \tau e_w + \frac{h(h_i f + h f_i)}{(h^2 + h_i^2)} e_{v_i} + \tau_i e_{w_i}$.

The choice of the frame $\mathbf{e}$ is such that $\mathbf{e}_z, \mathbf{e}_{z_i} \in \mathcal{D}^\perp$. For $\gamma'(0) \in \mathcal{D}$, we have $z(0) = z_i(0) = 0$ and since $\overset{A}{\nabla}$ restricts γ' to $\mathcal{D}$, the functions $z(t), z_i(t)$ will remain identically zero. Let us define $\eta_i \triangleq \frac{h_i(h_i f + h f_i)}{(h^2 + h_i^2)}$. The constrained dynamics of $\mathcal{A}$ in the frame $\mathbf{e}$ then reduce to

$$\begin{aligned} \dot{v} + v v_i \omega^v_{v_i v} + w v \omega^v_{vw} + w v_i \omega^v_{v_i w} + v_i v \omega^v_{v v_i} \ldots \\ \ldots + v_i v_i \omega^v_{v_i v_i} + w_i v_i \omega^v_{v_i w_i} = \eta_i \\ \dot{w} = \tau \\ \dot{v}_i + v v \omega^{v_i}_{vv} + v v_i \omega^{v_i}_{v_i v} + w v \omega^{v_i}_{vw} + v_i v \omega^{v_i}_{v v_i} \ldots \\ \ldots + w_i v \omega^{v_i}_{v w_i} + w_i v_i \omega^{v_i}_{v_i w_i} = \frac{h}{h_i}\eta_i \\ \dot{w}_i = \tau_i \end{aligned}$$

Notice that the constrained dynamics of the ith subsystem $\mathcal{A}$ in the $\mathbf{e}$ frame appear explicitly in the functions

$\mu_i, \dot{\mu}_i, q_i, \tau, \tau_i, \eta_i$ where $\mu_i = (v, w, v_i, w_i)$ and q_i is the configuration. The functions v, w, τ are the only common functions to appear in each of the N such subsystems. For consensus, we require these functions v, w, τ to have the same value at any given time in each of the N such subsystems. To ensure we have the same values for w, τ in each of the N subsystems simply means to have the same intrinsic(independent of the local coordinates q_i) control law for τ in each of them along with compatible initial conditions.

To ensure v has the same value in each of the N subsystems, consider the following control law for τ_i;

$$\tau_i = K_w(w_i^d - w_i) + \dot{w}_i^d \tag{8}$$

where $w_i^d = \frac{-vv_i\omega^v_{v_iv} - wv\omega^v_{vw} - wv_i\omega^v_{v_iw} - v_iv\omega^v_{vv_i} - v_iv_i\omega^v_{v_iv_i}}{v_i\omega^v_{v_iw_i}}$. The above control law that exponentially stabilizes w_i to w_i^d along with the initial condition $w_i(0) = w_i^d(0)$, reduces the first equation of constrained dynamics to $\dot{v} = \eta_i$. An intrinsic control law for f where $\eta_i = f, \forall i$ along with the above control law for τ_i ensures v has the same value in each of the subsystems. We develop two sets of intrinsic controllers for the functions τ and f; one to ensure *feasibility* and the other to achieve the *team goal*.

Controls for feasibility: Previous results of this same problem in [7] suggest that when $w = 0$, actuator and operating constraints are satisfied, thus ensuring feasibility. We use this observation without analysis or proof here and simply verify it in simulations. Consider the following controllers for the functions τ and f;

$$\tau = \begin{cases} -K_w w & if \quad |K_w w| \leq \tau^{max} \\ -sgn(w)\tau^{max} & else \end{cases} \tag{9}$$
$$f = 0$$

where the control law for τ asymptotically stabilizes w to zero, ensuring feasibility in the steady state. Future work will look at developing a control law that will result in feasibility in the transient states and hence guarantee true dynamic feasibility.

Controls for team goal: The team goal is to generate a phantom trajectory moving towards the desired waypoint. We translate this goal to the requirement of orienting the phantom UAV towards the desired waypoint and propose the following controllers to achieve this goal.

$$\tau = \begin{cases} K_w(w^d - w) + \dot{w}^d \;\; if \;\; |K_w(w^d - w) + \dot{w}^d| \leq \tau^{max} \\ sgn(K_w(w^d - w) + \dot{w}^d)\tau^{max} \quad else \end{cases}$$
$$f = \begin{cases} K_v(v^d - v) + \dot{v}^d \quad if \quad |K_v(v^d - v) + \dot{v}^d| \leq f^{max} \\ sgn(K_v(v^d - v) + \dot{v}^d)f^{max} \quad else \end{cases}$$

where, $v^d = \begin{cases} v^{min} & if \quad (\beta - \theta)\ is\ large \\ v^{max} & else \end{cases}$ and $\omega^d = K_{\beta-\theta}(\beta - \theta) + \dot{\beta}$, asymptotically stabilizing $(\beta - \theta)$ and $(v - v_d)$ to zero. Here $\beta = \tan^{-1}\left(\frac{y_f - y}{x_f - x}\right)$ with (x_f, y_f) being the desired waypoint of the Phantom. Physically, $(\beta - \theta)$ is the angle between the desired waypoint of the phantom and its current heading. In the control law for f, v^d is v^{min} when the angle $(\beta - \theta)$ is above a threshold value (i.e. when the phantom is not sufficiently oriented towards its final waypoint), and is v^{max} otherwise. The objective is to speed up the phantom UAV when oriented towards its desired waypoint and to slow down when not.

The distributed control architecture to generate reference trajectories implemented in a receding horizon approach is shown in the form of a flow-chart in Fig.(3). Each of the

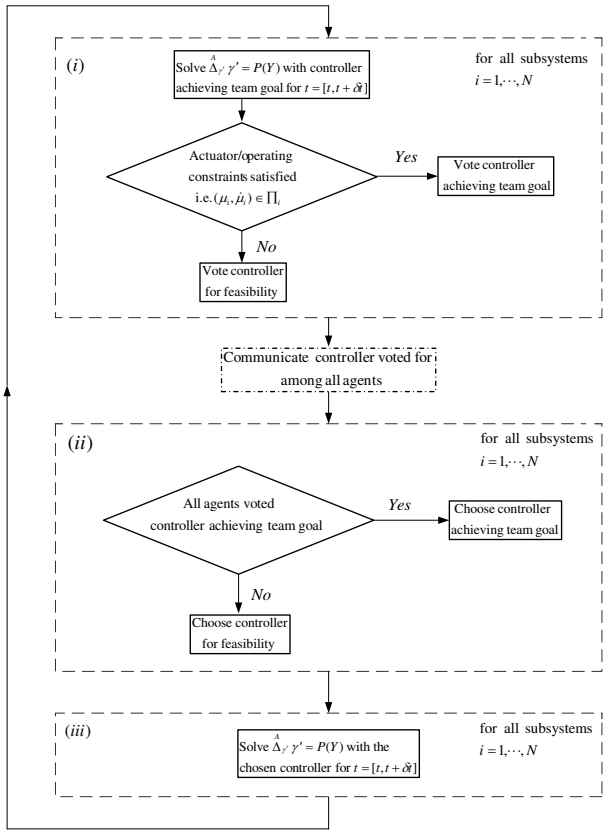

Fig. 3. Distributed control architecture.

N UAVs solves its corresponding constrained dynamics for the time interval $t = [t, t + \delta t]$ with controls to achieve the team goal first. Next they verify if all actuator/operating constraints $(\mu_i, \dot{\mu}_i) \in \Pi_i$ were satisfied for their corresponding subsystems during this time interval. Since constrained dynamics are solved in the functions μ_i, this step is straight forward. If all the actuator/operating constraints were satisfied in a particular subsystem, the corresponding UAV votes for the controls achieving the team goal. If any of the actuator/operating constraints were violated within $[t, t+\delta t]$, the UAV votes for the controls for feasibility. Recall that each of the subsystems need to implement identical control actions for τ, f for consensus. Hence each of the N UAVs communicates the type of controller it voted for and the entire team of UAVs picks a common controller type to implement for the horizon interval $[t, t + \delta t]$. If all the N UAVs had

voted for the controller achieving the team goal, then each of the N UAVs, and hence the entire team of UAVs, chooses and implements controls for the team goal to compute its trajectory. Else, all of the N UAVs chooses controls for feasibility to solve the constrained dynamics for $[t, t+\delta t]$. The algorithm then incrementally steps forward in δt time steps, until the phantom track reaches its desired waypoint. A necessary redundancy in the proposed distributed control architecture is that each of the N UAVs designs the phantom trajectory in addition to its own trajectory. This algorithm is scalable since the computations shown in the blocks (i), (ii) and (iii) of the flow-chart of Fig.3 are performed by each of the N UAVs in parallel and as such increasing the number of agents in the system has minimal effect on the overall computation time. Communication amongst the agents need not be continuous and has to occur only once in each iteration. A severe drawback of this strategy however is that it requires synchronized control and communication among all its agents.

III. Simulation Results

Simulation results of this algorithm for the case of 4-UAVs engaging 4-radars are shown in Fig.4. Actuator and operating constraints on the phantom and the individual UAVs were assumed as follows. Phantom speed of $400 \pm 40m/s$, UAV speeds of $100 \pm 15m/s$ and minimum turn radii of $5000m$ and $1500m$ for the phantom and the UAVs, respectively. Force and toque bounds of $[-0.7N, 0.7N]$ and $[-0.04Nm, 0.04Nm]$ respectively for the phantom as well as the UAVs. The force and torque are normalized quantities with the unit mass, unit inertia assumption. The time history

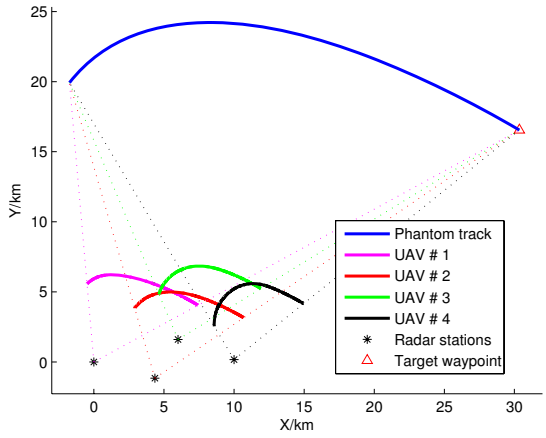

Fig. 4. Four UAVs deceiving a radar network of four radars through the generation of a phantom track.

of the functions v, w, v_i, w_i corresponding to "speed" and "steer" of the UAVs and the phantom are shown in Fig.5, for the trajectory results of Fig.4. The lower and upper bounds of v, w, v_i, w_i are also shown. The normalized torque and force corresponding to each of the four UAVs and the phantom UAV are illustrated in Fig.6 and here it is seen that the forces

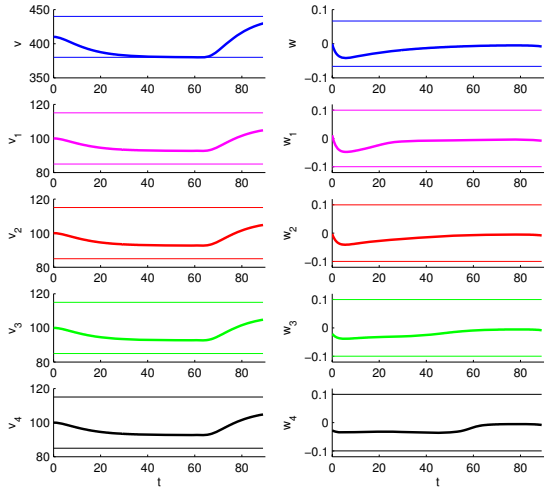

Fig. 5. Speed and steer, along with their upper and lower bounds, for each of the four UAVs and the UAV representing the phantom.

f_i and f are identically the same. This is since the control

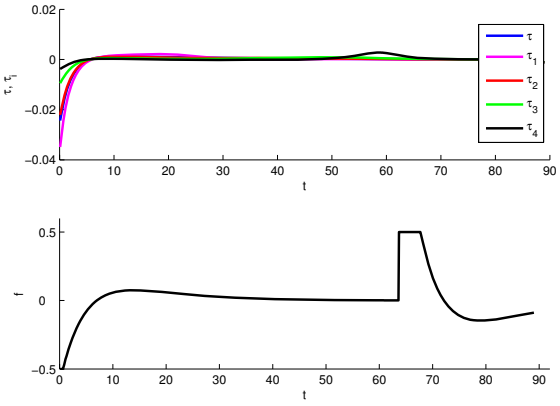

Fig. 6. Torque and force control functions, for each of the four UAVs and the UAV representing the phantom.

law for τ_i, given by Eq.(8), apparently forces $\frac{v_i}{v}$ to remain the same constant value. This is verified in Fig.7 which plots the ratios $\frac{v_i}{v}$ and $\frac{r_i}{R_i}$ against time for each of the UAVs, where r_i is the distance from the ith UAV to its corresponding radar and R_i is the distance from the phantom to the same radar. As can be seen in Fig.7, the ratio $\frac{v_i}{v}$ remains constant against time while the ratios of $\frac{r_i}{R_i}$ all converge to it. This is a phenomena which was explained in the kinematic analysis of the radar deception problem presented in [7]. There it was shown that the convergence of $\frac{r_i}{R_i} \rightarrow \frac{v_i}{v}$ reduces the dynamics of the multi-agent system to the dynamics of a single UAV, controllable on its configuration submanifold. In other words, all the four UAVs converge to a seemingly stable rigid formation maintaining parallel motion. The rigid

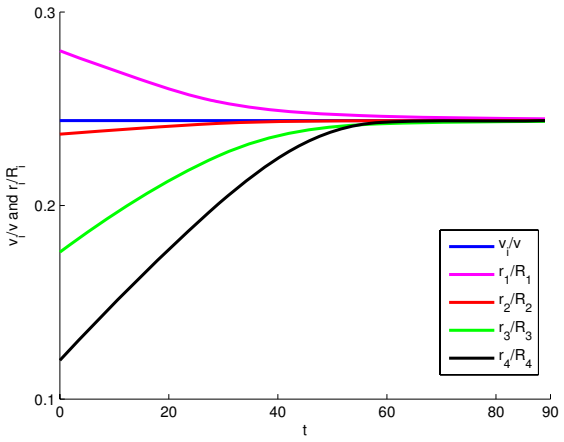

Fig. 7. The ratios of $\frac{v_i}{v}$ and $\frac{r_i}{R_i}$ for the four UAV-radar pairs.

formation it converges to is a contracted geometric copy (contracted by a factor of $\left(1-\frac{v_i}{v}\right)$) of the geometric formation of the ground radar network. If all four UAVs were to start out with initial conditions such that $\frac{r_i}{R_i}=\frac{v_i}{v}$, then the phantom UAV is controllable with all the UAVs in parallel motion, maintaining a rigid formation. This case is illustrated in Fig.8.

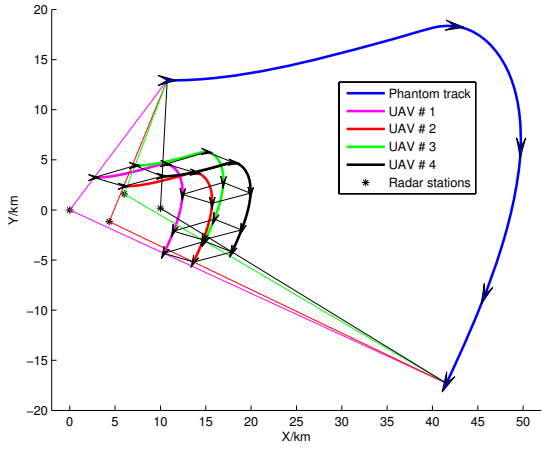

Fig. 8. Parallel motion of four UAVs maintaining a stable rigid formation, for initial conditions satisfying $\frac{r_i}{R_i}=\frac{v_i}{v}$.

The real-time corresponding to the trajectories shown in Fig.4 with $\delta t = 1\,\text{sec}$ was $89\,\text{sec}$ while the CPU time (computation time) of each of the UAVs in the distributed control architecture was $7.5\,\text{sec}$.

IV. Conclusion

This paper presents a motion planning algorithm producing dynamically feasible reference trajectories in real-time for the radar deception problem. Trajectory tracking controllers available in the literature are then to be used by each UAV to track these reference trajectories. Robustness to model uncertainty and external disturbances will come through these tracking control laws which will be based on feedback control. A notable weakness in this algorithm however is in the synchronized communication; unrealistic due to inevitable time-delays. Asynchronous communication, robustness in the communication topology, time-delays and other important issues will need to be addressed before this algorithm can be implemented on an actual multi-agent test bed. However it is emphasized here that this algorithm is meant more to convince the need for a paradigm change in formation control that respects realistic dynamic constraints than for operational significance.

Some of the key attributes of the motion planning algorithm verified through simulations for the radar deception problem are: (i) designs dynamically feasible reference trajectories (ii) scalable (iii) suited for real time computation (iv) communication (time and data) between agents is small (v) implementable as an autonomous team of agents (vi) the receding horizon approach has a feedback structure providing inherent robustness in the design of reference trajectories.

References

[1] K.B. Purvis, P.R. Chandler, and M. Pachter, "Feasible Flight Paths for Cooperative Generation of a Phantom Radar Track," *Proc. of AIAA Guidance, Navigation, and Control Conference*, Providence, RI, 2004.

[2] M. Pachter, P.R. Chandler, Reid A. Larson, K.B. Purvis, "Concepts for Generating Coherent Radar Phantom Tracks using Cooperative Vehicles," *Proc. of AIAA Guidance, Navigation, and Control Conference*, Providence, RI, 2004.

[3] D.H.A. Maithripala and S. Jayasuriya, "Radar Deception Through Phantom Track Generation," *Proc. of 2005 American Control Conference*, Portland, OR, 2005, pp. 4102-4106.

[4] K.B. Purvis, P.R. Chandler, and M. Pachter, "Feasible Flight Paths for Cooperative Generation of a Phantom Radar Track," J. Guid. Control Dyn., 29(3), 2006, pp. 653-661.

[5] M.J. Mears, "Cooperative Electronic Attack Using Unmanned Air Vehicles," *Proc. of 2005 American Control Conference*, Portland, OR, 2005, pp. 3339-3347.

[6] D.H.A. Maithripala, S. Jayasuriya, M.J. Mears, "Real-Time Control of an Autonomous Control System Based on Feasibility Analysis," *Proc. of the 45th IEEE Conference on Decision and Control*, San Diago, CA, 2006, pp.4277-4282.

[7] D.H.A. Maithripala, S. Jayasuriya, M.J. Mears, "Phantom Track Generation through Cooperative Control of Multiple ECAVs Based on Feasibility Analysis," ASME J. of Dyn. Syst., Meas., Control, vol. 129, 2007, pp. 708-715.

[8] K.B. Purvis, P.R. Chandler, "A Review of Recent Algorithms and a New and Improved Cooperative Control Design for Generating a Phantom Track", *Proc. of 2007 American Control Conference*, Portland, NY.

[9] D.H.A. Maithripala, S. Jayasuriya, "Phantom Track Generation in 3D through Cooperative Control of Multiple ECAVs Based on Geometry," *Proc. of the First International Conference on Industrial and Information Systems*, Peradeniya, Sri Lanka, 2006, pp.255-260.

[10] D.H.A. Maithripala, D.H.S. Maithripala, S. Jayasuriya, "Unifying Geometric Approach to Real-time Formation Control," *Proc. of 2008 American Control Conference*, Seattle, WA, 2008.

[11] F. Bullo and A. Lewis, *Geometric Control of Mechanical Systems*, ser. Number 49 in Texts in Applied Mathematics. Springer-Verlag, 2004.

[12] T. Frankel, *The Geometry of Physics: An Introduction*. Cambridge University Press, 1997.

[13] A.D. Lewis, "Simple mechanical control systems with constraints," IEEE Transactions on Automatic Control, 45(8), 2000, pp. 1420-1436.